Astron. Astrophys. 288, 929–941 (1994)

ASTRONOMY
AND
ASTROPHYSICS

Dust in protostellar cores and stellar disks

E. Krügel[1] **and R. Siebenmorgen**[2]

[1] Max-Planck-Institut für Radioastronomie, Auf dem Hügel 69, D-53121 Bonn, Germany
[2] ISO Science Team, Astrophysics Division, Space Science Dept, ESTEC, Postbus 299, NL-2200AG Noordwijk, The Netherlands

Received 8 January 1994 / Accepted 10 March 1994

Abstract. We present the absorption and extinction cross section κ as a function of wavelength for dust that is thought to exist in cold dense clouds as well as in stellar disks. The grains are fluffy and composed of subparticles of astronomical silicate and amorphous carbon with an admixture of frozen ice. We assume a grain size distribution $n(a) \propto a^{-3.5}$ with fixed lower limit $a_- = 300$Å and variable upper limit a_+.

Particular attention is given to the cross sections at $2.2\mu m$ and $1.3mm$, as these are the wavelengths for detecting embedded young stars and deriving masses from dust emission. As long as the grains are smaller than $100\mu m$, which must apply to the cores of cold protostellar clouds, the absorption coefficient at $1.3mm$ is about $0.02\,cm^2$ per g of interstellar matter, an enhancement by a factor of eight relative to the diffuse interstellar medium; its variation with frequency is $\kappa \propto \nu^2$ in the submm/mm region. At $2.2\mu m$, the optical depth increases by a factor of 1.5 if the grains are small ($a_+ < 1\mu m$). Should coagulation have increased their size the outcome depends sensitively on the precise value of a_+.

We show in detail how variations in grain size, fluffiness and ice mantle affect the cross section and also the temperature that grains acquire in a far IR radiation field. We also discuss the dust around Vega–type stars where the largest grains are known to be several millimeters big.

Key words: interstellar medium: dust – circumstellar matter

1. Introduction

The dust in dense clouds is certainly different from the dust in the diffuse medium. This is best witnessed by changes in the extinction curve: In dense clouds, the ratio of UV to visual extinction is usually much smaller. The basic process for this modification is probably grain coagulation which leads to fluffy particles as advocated by Mathis & Whiffen (1989). In compact regions the number of small particles, responsible for the UV absorption, is reduced and the mean grain size increases. Measurements of the extinction curve are, however, for reasons of sensitivity restricted to moderate optical depth and one can only extrapolate to the conditions in heavily obscured regions.

The second important process in dense clouds, besides coagulation, is the formation of ice mantles which are composed of molecules like H_2O, NH_3, CO, ... (Tielens et al. 1991; Whittet 1993; van Dishoeck et al. 1993) and possibly contain as impurities polycyclic aromatic hydrocarbons (PAH; Allamandola et al. 1989). Ice mantles form in a weak radiation field and at low grain temperatures and are observed through the absorption of individual molecular groups, best known is the OH stretching in H_2O at $3.1\mu m$. The physics of ice mantle are complicated and not well understood. Frozen out atoms or molecules may further react in the mantle to form new compounds. If activation barriers have to be overcome, the energy input from the environment (energetic photons, cosmic rays) is obviously important for the chemical composition of the mantle. The properties of the ice depend also on the mixing ratio of the molecules in the solid, on the degree of impurity and on the grain temperature as warming enables the molecules to arrange differently. Evidently, ice mantles must be quite heterogeneous.

Another piece of evidence for the change of grain properties in dense clouds comes from estimates of the gas mass M_g as derived from molecular lines and from the millimeter radiation of dust. Whereas the two values usually agree within a factor of three, for some objects of high density one derives from the dust a *much* greater gas mass than from optically thin molecular lines. A striking example is the cold cloud fragment HH24 MMS in L1652 (Chini et al. 1993; Krügel & Chini 1994), where this discrepancy exceeds two orders of magnitude.

In the past years, extensive efforts have been made to explore the properties of fluffy grains as well as the coagulation and growth processes (Morfill 1984; Witten & Cates 1986; Meakin & Donn 1988; Wright 1988; Kozasa et al. 1992; Chokshi et al. 1993; Blum et al. 1993; Ossenkopf 1993). For understanding extinction and emission in dense clouds, a proper description of the interaction of light with this kind of matter is required. In this paper, we investigate how coagulation and ice accretion in-

Send offprint requests to: E. Krügel

fluence the dust in cold and dense environments and we address the following questions relevant to the study of star formation:

a) How does the mass absorption coefficient, $\kappa^{abs}_{1.3mm}$, at $1.3mm$ change? This wavelength is widely used for mass estimates because the optical depth of the atmosphere is low and the dependence of the Planck function on temperature is weak. There is an obvious need to determine $\kappa^{abs}_{1.3mm}$ well because it is inversely proportional to the dust mass M_d and, provided the dust–to–gas ratio is constant, also to the gass mass.

b) How is the $2.2\mu m$ extinction coefficient, $\kappa^{ext}_{2.2\mu m}$ altered? The wavelength of $2.2\mu m$ (K-band) is favored in searches for enshrouded embryo stars because the optical depth is much lower than in the visual, the atmosphere is transparent and the dust is generally not hot enough ($\leq 1000K$) to radiate itself.

c) How are the dust temperature T_d and estimates of it affected? T_d itself is not a directly observable quantity. Dust continuum observations only yield a color temperature T_c via a flux ratio at two wavelengths. This question is intimately related to the assumption about the submm wavelength dependence of κ_ν, usually written as $\kappa_\nu \propto \nu^\beta$.

d) As T_d follows from the balance between absorbed and emitted energy, its calculation involves the absorption coefficient κ^{abs}_λ at all wavelengths. This naturally leads to the question: What are realistic values for a mixture of fluffy and icy particles?

2. Tools for calculating cross sections

2.1. Realistic grain structure

The solid particles in cold and dense clouds or in stellar disks are probably *fluffy aggregates*, substantially bigger than normal interstellar grains. They are composed of two kinds of refractory subparticles: astronomical silicate and amorphous carbon (aC), hereafter simply silicate and carbon. The subparticles are compact and their size need not be specified in the calculations, but we imagine them to have diameters of a few hundred Angstrom; the coagulated grain is, of course, bigger. The process of coagulation is accompanied or has been preceded by the frosting of molecules to form ice layers on the surface of the subparticles. So we envisage the grains to consists of four components with distinct optical constants: silicate, carbon, ice and vacuum in between. Their possible diversity is infinite and their true structure must be extremely complex. We call them in the following "realistic" grains.

For the specific weight of the refractory subparticles we take a uniform value $\rho_{ref} \approx 2.5 g\,cm^{-3}$. The volume ratio of silicate to carbon material in the grain is $f^{Si}/f^C = 1.41$ and follows from the usual cosmic abundances in solids. The subparticles are ice–coated and the ice mantle has a specific weight $\rho_{ice} \approx 1 g\,cm^{-3}$. The available mass of condensible material is determined by the gas phase abundances of C, N and O and their hydrides. Using standard values, the maximum ratio of volatile to refractory mass, M_{ice}/M_{ref}, is somewhere between 1 and 2. Consequently, the ice volume may be several times bigger than the volume of the refractories.

2.2. Optical constants

Besides the particle structure, the other important quantity is the wavelength dependent optical constant, $m = n - i \cdot k$, of each grain component. When calculating cross sections over the whole spectrum we use for silicate data after Draine (1985), for carbon (aC) after Rouleau & Martin (1991) and for ice after Preibisch et al. (1993). None of the optical constants for ice or carbon extends beyond the submm region so values for longer wavelengths have to be extrapolated.

As we study in detail the dust cross section at $2.2\mu m$ and $1.3mm$ we remark briefly on the optical constants that we use at these wavelengths in Figs. 1 to 11. For carbon and ice, they may not exactly coincide with the tables of Rouleau & Martin (1991) and Preibisch et al. (1993), but the deviations are of no relevance; they arise for historical reasons from extrapolation and interpolation among various tables (of Edoh 1983; Bussoletti et al. 1987; Blanco et al. 1991 and Preibisch et al. 1993 for carbon; of Bertie et al. 1969 and Leger et al. 1983 for ice).

At $1.3mm$, $m_{Si} = 3.5 - i \cdot 0.05$ and $m_{aC} = 16.5 - i \cdot 14.1$ which agrees with the value of Edoh at $905\mu m$. In the optical constant of ice, the decisive quantity is the impurity expressed by k_{ice}; the refractive index n_{ice} is not critical. Pollution can come from metal atoms or tiny particles, but its degree is uncertain. Preibisch et al. (1993) calculate from effective medium theory $k_{ice}(800\mu m) = 0.024$ if 10% of the mantle volume is polluted by carbon; Bertie et al. (1969) give at $330\mu m$ $n_{ice} = 1.79$ and $k_{ice} = 0.024$. We adopt $n_{ice} = 1.7$ and consider k_{ice} a free parameter.

At $2.2\mu m$, $m_{Si} = 1.71 - i \cdot 0.034$ and $m_{aC} = 2.7 - i \cdot 1.0$. The carbon value is again after Edoh (1983), other authors give k–values some 20% lower. With respect to ice, we assume $n_{ice} = 1.23$ (Leger et al. 1983). Exactly as at $1.3mm$, the uncertainty lies in the degree of mantle pollution. Leger et al. (1983) recommend for amorphous ice $k_{ice} = 0$, Bertie et al.(1969) for crystalline ice $k_{ice} = 5 \cdot 10^{-4}$ and Preibisch et al. (1993) for a mantle polluted by tiny carbon particles $k_{ice} = 0.044$. Because of these discrepancies we again allow k_{ice} to vary.

In the picture of Preibisch et al., k_{ice} is not a free parameter. They assume that pollution of ice comes from PAHs and very small carbon grains, which can at best account for 20% of the carbon mass. Therefore, if they are completely built into the ice an increase in ice mass only dilutes the pollutant per unit volume. For example, for $M_{ice}/M_{ref} = 1$ and adopting $k_{ice} \propto \lambda^{-1}$ for $\lambda > 800\mu m$, according to Preibisch et al. k_{ice} at $1.3mm$ cannot be greater than 0.006. However, we allow it to be larger. First, we take the view that k_{ice} is at present not so well known. Second, it turns out in the calculations of composite particles (Sect. 4.1) that the volume fraction of amorphous carbon is not very important for the final absorption cross section. So if *most* of the carbon is considered to be polluting the ice (not only PAHs), then the degree of pollution (k_{ice}) is several times higher; the volume fraction of amorphous carbon (refractory component) is then, of course, correspondingly lower, but with little effect on the absorption cross section.

2.3. Computational methods

All subsequent computations of the absorption and extinction efficiencies are performed with Mie theory described, for example, by Kerker (1969). It is an exact theory based on classical electrodynamics for a continuous medium. Mie calculations are numerically fairly simple, however, very idealized grain geometries have to be assumed, usually spheres.

For fluffy grains there are no exact, but only approximate methods of calculating cross sections. A numerical simple and often satisfactory tool is given by the effective medium theories of Maxwell–Garnett or Bruggeman (Jones 1988; Mathis & Whiffen 1989; Ossenkopf 1991). Here it is envisaged that the particle consists of a matrix with inclusions that are much smaller than the wavelength λ. The complex dielectric constants of the matrix ϵ_m and the inclusion ϵ_i are combined into an average ϵ_{av} which is then used in the Mie formalism; the shape of the particles is assumed to be spherical. Let the indices i and m refer to inclusion and matrix, respectively, let ϵ denote the dielectric constant and f the volume fraction. If there is only one kind of inclusions the dielectric constant averaged over the whole grain, ϵ_{av}, is found after Bruggeman from the equation

$$f_i \cdot \left(\frac{\epsilon_i - \epsilon_{av}}{\epsilon_i + 2\epsilon_{av}} \right) + f_m \cdot \left(\frac{\epsilon_m - \epsilon_{av}}{\epsilon_m + 2\epsilon_{av}} \right) = 0 \qquad (1)$$

and after Maxwell–Garnett from

$$\epsilon_{av} = \epsilon_m \cdot \left(1 + \frac{3 f_i \cdot (\epsilon_i - \epsilon_m)/(\epsilon_i + 2\epsilon_m)}{1 - f_i \cdot (\epsilon_i - \epsilon_m)/(\epsilon_i + 2\epsilon_m)} \right) \qquad (2)$$

with the obvious condition: $f_i + f_m = 1$. The average optical constant $m_{av} = n - ik$ ($k > 0$) to be used in the Mie theory follows from $\epsilon_{av} = m_{av}^2$.

Both theories may readily be extended to multicomponent mixtures (Bohren & Huffman 1983). This generalization is important because the grains that we consider are a mixture of silicate, carbon, ice and vacuum. However, only the Bruggeman rule is symmetric with respect to the components, whereas in the Maxwell–Garnett rule one has to specify which of them constitutes the matrix. (For a discussion of the theories see Bohren & Huffman (1983) or Ossenkopf (1991)). We favor the Bruggeman rule for the practical reason that it exempts us from assigning the matrix, especially as all components have more or less comparable volume fractions. But as we are not certain which theory is better suited for our purposes we present results from both.

Alternatively, the absorption of a fluffy particle that consists of *one* chemical component with vacuum inclusions may be evaluated with Mie theory for a hollow sphere: An inner spherical cavity ($m_i = 1$) is encompassed by a shell. This case may be considered as a matrix with only one vacuum inclusion; we show results in Figs. 6 and 7.

3. The modifications of dust in cold and dense clouds

A cold and dense environment changes the dust in three major ways: It increases the grain size, produces fluffy structures and leads to ice coating. These are complicated and time-dependent processes and each of them modifies the cross section. Although the modifications will occur simultaneously, in this section we study them separately. This helps us to better understand them and to evaluate their relative importance.

3.1. Big solid grains

One major feature of heavily coagulated particles is their larger size. Therefore we compute the cross section of large grains as a function of radius a. This is done under the assumption that they are uncoated solid spheres of uniform chemical composition. Because we are interested how the cross section of the dust changes in dark clouds or disks with respect to the diffuse medium we present a normalized value obtained in the following way: We calculate the cross section of $1g$ of dust consisting of identical grains, all of (large) radius a and divide it by the cross section of $1g$ of dust of the same chemical composition, but where the grains have a standard MRN size distribution, $n(a) \propto a^{-3.5}$, (Mathis et al. 1977) with lower and upper grain radius $a_- = 100$Å and $a_+ = 3000$Å, respectively. The normalized value is denoted by $\mathscr{K}$, or $\mathscr{K}_\nu(a)$ to indicate the dependence on frequency ν and on grain radius a.

3.1.1. The 1.3mm absorption coefficient of big grains

As long as the grains are much smaller than the wavelength λ, the normalized mass absorption coefficient, $\mathscr{K}^{abs}$, is independent of grain size (Rayleigh limit). Figure 1 shows $\mathscr{K}^{abs}$ at $1.3mm$ as a function of radius a for both silicate and carbon. $\mathscr{K}$ is unity, i.e. there is no increase in the absorption coefficient relative to the standard dust, as long as the silicate particles are smaller than $30\mu m$ and the carbon particles smaller than $1\mu m$. When the grains are much bigger than the wavelength, $a >> \lambda$, the absorption efficiency attains some constant value $Q \leq 1$ and $\mathscr{K}$ decreases inversely with radius:

$$\mathscr{K}_\nu(a) \propto \frac{\pi a^2 Q_\nu}{\frac{4\pi}{3}\rho_d a^3} \propto a^{-1} \qquad (3)$$

ρ_d being the density of the grain material. In principle, Mie calculations are necessary only for the intermediate range where $2\pi a \approx \lambda$, but there the changes are impressive. For both silicate and carbon, $\mathscr{K}$ rises by a factor 10 or more because grains with $a \approx \lambda$ are much better radiators than smaller particles. For silicates, the increase sets in suddenly and values substantially greater than one are realized in the range from $a = 100 \ldots 3000\mu m$. Silicates also show resonances at particular radii; they would, however, be smeared out in a size distribution. For carbon, $\mathscr{K}$ is noticeably enhanced if a is between 5 and 500 μm.

3.1.2. The $2.2\mu m$ extinction coefficient of big grains

For estimating the visibility of a dust enshrouded object at $2.2\mu m$ we have to take into account not only absorption, but also scattering. Therefore we plot in Fig. 2 in addition to the

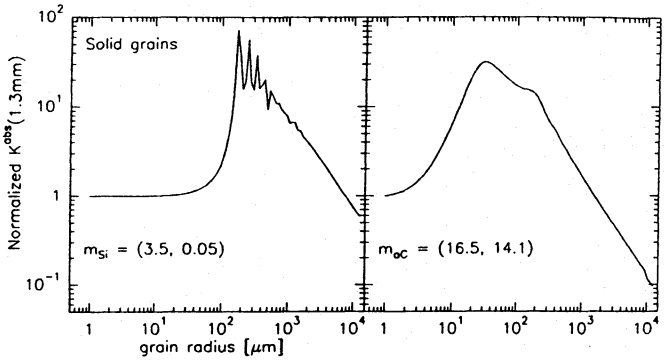

Fig. 1. Normalized absorption cross section at $1.3mm$ as a function of grain radius. The grain is an uncoated solid sphere of uniform chemical composition either made of astronomical silicate (*left*) or amorphous carbon (*right*). Optical constants are indicated, for normalization see Sect. 3.1

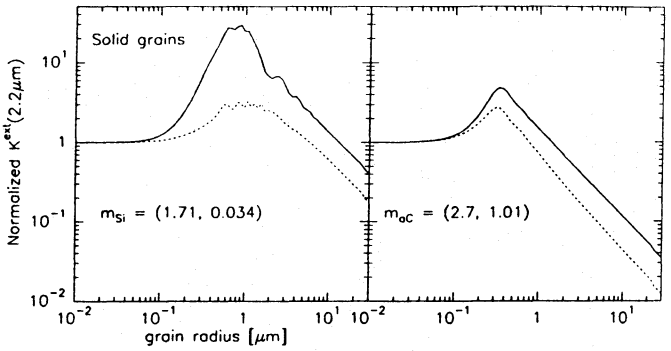

Fig. 2. Normalized cross section for extinction (solid line) and absorption (dashed line) as a function of grain radius at $2.2\mu m$. See also Fig. 1

normalized absorption coefficient also the normalized extinction as a function of grain radius. Scattering by itself does not remove a single photon, but it increases the path length and thus the probability for absorption. Despite the difference in optical constants, the qualitative behavior of $\mathscr{K}$ at $2.2\mu m$ is similar to that at $1.3mm$: For small a, $\mathscr{K}$ equals one; it rises at intermediate radii and falls off proportionally to a^{-1} for large grains. Eventually it drops to values below those of normal interstellar dust. For silicates, the maximum in $\mathscr{K}$ is broad, reaching almost 30 (!) shortly before $a = 1\mu m$. $\mathscr{K}$ becomes noticeably bigger than 1 when $a > 0.1\mu m$. Carbon particles are even smaller ($\approx 0.3\mu m$) when they reach their maximum. Such sizes are already encountered among normal interstellar grains, but then, of course, only as the tail of the size distribution.

3.1.3. Temperatures of big grains

The size of a particle also affects the temperature T_d which it attains in a radiation field J_ν. This becomes obvious from the equation for the balance between emitted and absorbed energy

$$\int J_\nu Q_\nu^{abs}(a)\, d\nu = \int B_\nu(T_d) Q_\nu^{abs}(a)\, d\nu \qquad (4)$$

We illustrate how T_d depends on the grain radius a in the case of a far IR field without a UV component, the kind that prevails in the core of a dark cloud. With regard to the spectral shape we choose for the sake of simplicity diluted black body emission, $J_\nu \propto B_\nu(T_{rad})$, of temperature $T_{rad} = 30K$ and $100K$; the intensity has then its peak around $50\mu m$ and $160\mu m$, respectively. Let the integrated flux $\int J_\nu d\mu$ be the same for both fields. In Fig. 3 the solid line refers to silicate, the dashed line to carbon. For $a < 1\mu m$, i.e. for all grains of standard size, T_d is almost constant. It declines for larger radii and levels off when $a > 30\mu m$. The absorption efficiency of very big grains approaches a value slightly below one; it is not exactly unity because the particle has an albedo. Nevertheless, large grains behave very much like black bodies which have $Q_\nu = 1$ and are always cooler than real particles. In the radiation field of 100K, the very big grains are much colder than standard interstellar ones, by a factor of two. For the radiation field with $T_{rad} = 30K$, the slump in T_d is less dramatic because the average wavelengths are now larger and the grains do not yet resemble black bodies. We point out that the results would be quite different for a UV radiation field.

We next ask what color temperature T_c one would derive observationally not knowing that the grains are big. T_c is obtained for optically thin emission from the flux ratio S_1/S_2 at two wavelengths λ_i (i=1,2)

$$\frac{S_1}{S_2} = \frac{\kappa_1 \cdot B_1(T_c)}{\kappa_2 \cdot B_2(T_c)} \qquad (5)$$

where κ_i is the absorption coefficient and $B_i(T_c)$ the Planck function. The true grain temperature ($T_c = T_d$) follows only if in Eq.(5) the correct ratio κ_1/κ_2 is inserted; otherwise the color temperature has no physical meaning. Let us consider the wavelengths $\lambda_1 = 450\mu m$ and $\lambda_2 = 1300\mu m$ as they are appropriate for determining T_c in a cold cloud. Assuming $\kappa_\lambda = \lambda^{-m}$, usually with $m \simeq 2$ for standard dust, one obtains $(\kappa_{450}/\kappa_{1300})_{sta} = 8.35$, whereas very large grains have $\kappa_{450}/\kappa_{1300} \simeq 1$. The radii where $\kappa_{450}/\kappa_{1300}$ becomes different from $(\kappa_{450}/\kappa_{1300})_{sta}$ can be read off Fig. 1: it is at $a \approx 20\mu m$ for silicates and at $a \approx 1\mu m$ for carbon. In a mixture of silicate and carbon, the smaller of these two radii ($a \simeq 1\mu m$) would set the limit for the applicability of the usual method (Eq.(5)) to derive dust temperatures.

3.2. Solid grains with ice mantles

In dense clouds and at temperatures below 20K, all molecules that are considered important for ice mantles (H_2O, NH_3, CH_4, CH_3OH, CO, CO_2, ...) are expected to be frozen out or, at least, heavily depleted. The time scale for condensation, assuming a sticking coefficient of 1 in collisions between molecules and grains, is $\tau_{cond} \simeq 3 \cdot 10^9/n(H)$ years. At hydrogen densities $n(H) > 10^5\, cm^{-3}$, τ_{cond} is shorter than the dynamical time scale of a gravitationally unstable cloud. So if condensation is very effective it will prohibit the study of protostellar evolution with molecular spectroscopy.

In this section, we assume normal grain sizes and a radius of the refractory core $a_{core} = 10^{-5}\, cm$. As core mate-

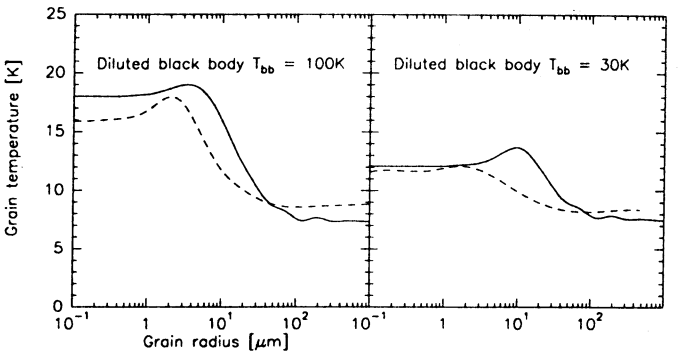

Fig. 3. Grain temperature as a function of grain radius for solid spheres made of silicate (solid line) or amorphous carbon (dashed line). The grains are embedded in a diluted black body radiation field of T = 100 K (*left*) and T = 30 K (*right*); see Sect. 3.1.3

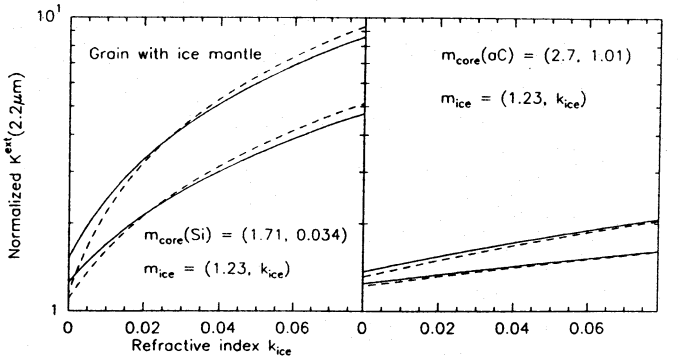

Fig. 5. Normalized extinction (solid lines) and absorption (dashed lines) cross section at 2.2 μm of ice coated grains as a function of the imaginary part k_{ice} of the refractive index of the ice mantle; *left:* silicate core, *right:* carbon core. See Fig. 4

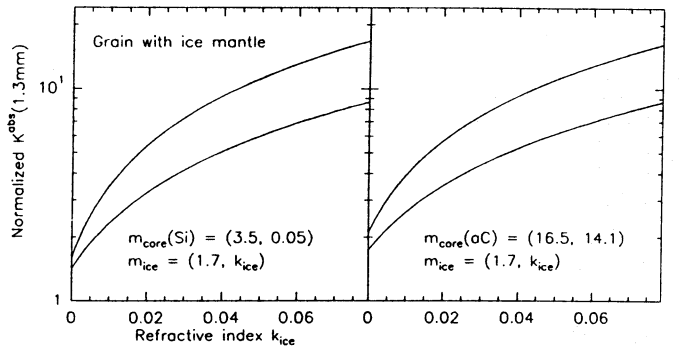

Fig. 4. Normalized absorption cross section at $1.3mm$ of ice coated grains as a function of the imaginary part k_{ice} of the refractive index of the ice mantle. The core has a radius $a_{core} = 0.1\mu m$ and consists either of silicate (*left*) or carbon (*right*). The upper curves refer to an ice mass equal to the mass of the refractory core, $M_{ice}/M_{ref} = 1$, the lower ones to $M_{ice}/M_{ref} = 0.5$; the corresponding ratios of outer–to–core radius are $a_{coat}/a_{core} = 1.52$ and 1.31, respectively. For normalization see Sect. 3.2

rial we take again carbon and silicate. For the mass ratio of the volatile ice to the refractory core we choose rather conservatively $M_{ice}/M_{ref} = 0.5$ and 1. Given the specific weight of core and mantle (2.5 and 1 g/cm^3, respectively) this implies that the radius a_{coat} of the coated grain is 1.31 (1.52) times bigger than a_{core} (see Sect. 2.1); this result is only very weakly dependent on the choice of a_{core}. (In reality, the ratio a_{core}/a_{coat} is probably not uniform, but diminishes with particle size: Once a thin ice layer has formed, further condensation is not influenced by the core surface so that all mantles should have a uniform thickness independent of a_{core}.)

We normalize our results (Figs. 4 and 5) in the same spirit as we did for big grains. It basically amounts to dividing the cross section of the coated grain by that of the core alone. (More precisely, the cross section of coated grains, all of radius a and with a total core mass of $1g$, is divided by the cross section of $1g$ of dust of the same material as the cores, but where the grains have a standard MRN size distribution.)

3.2.1. The 1.3mm absorption coefficient of ice coated grains

When molecules freeze out the $1.3mm$ dust absorption coefficient rises. Figure 4 shows how $\mathscr{K}_{1.3}$ changes as a function of impurity. Accretion increases the cross section ($\mathscr{K} > 1$) even if the mantle is a pure dielectric ($k_{ice} = 0$) because some of the light impinging on the mantle is refracted into the absorbing core. $\mathscr{K}$ rises steadily with k_{ice}. For the educated guess $k_{ice} = 0.02$ and $M_{ice}/M_{ref} = 1$, the absorption coefficient is a factor of more than five above the uncoated dust. If k_{ice} is not small (≥ 0.02), doubling the ice volume roughly doubles $\mathscr{K}$ as can be seen by comparing the upper and lower curves. When we stretch M_{ice}/M_{ref} to 1.5, which is not at all unrealistic, and k_{ice} to 0.03 we see that coating alone can increase the dust absorption coefficient tenfold. Altogether, there is not much difference whether the core consists of carbon or silicate.

3.2.2. The $2.2\mu m$ extinction coefficient of ice coated grains

At $2.2\mu m$, the overall effect of ice mantles resembles the situation at $1.3mm$. In Fig. 5, k_{ice} is again a free parameter, but we think that $k_{ice} = 0.02$ is not a bad guess. The solid curves now refer to extinction, the dashed to absorption. They are both normalized to uncoated grains and thus have different normalization factors. Therefore the absorption line may lie above the extinction line although by definition extinction is always greater than absorption. Contrary to the situation at $1.3mm$, the core material makes a big difference: the ice mantle is much more important in case of a silicate core. Ice coated grains are also better scatterers at $2.2\mu m$. For $k_{ice} = 0$ and silicate cores, the albedo is substantial ($Q^{sca}/Q^{abs} \approx 0.5$), the precise ratio depends on the mantle thickness. As k_{ice} increases, scattering looses its importance. The effect of the mantle thickness is displayed by comparing in each frame the two solid lines. We conclude that at $2.2\mu m$ frosting of molecules can increase the extinction optical depth by a factor of two or more.

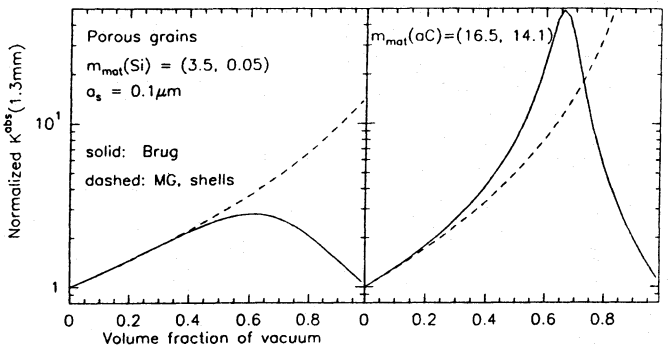

Fig. 6. Normalized absorption cross section at $1.3mm$ as a function of porosity. Computations are given for spheres consisting of silicate (*left*) and amorphous carbon (*right*). The spheres have a constant mass; when $f_{vac} = 0$ the grain radius is $a_s = 0.1\mu m$. The optical constant of the matrix material m_{mat} is indicated. Results are shown for three approximations: Bruggeman rule (solid line), Maxwell–Garnett rule (dashed) and hollow spheres (also dashed, the latter two approximations coincide)

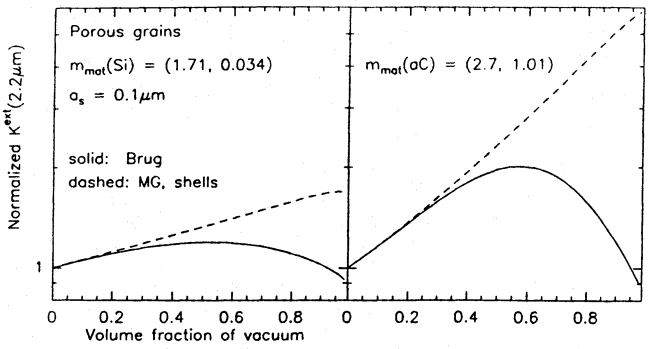

Fig. 7. As Fig. 6, but for the extinction cross section at 2.2 μm

3.2.3. Temperatures of ice coated grains

Evaluating the temperature of coated and uncoated grains from Eq.(4) for a far IR radiation field we find that an ice mantle changes T_d only marginally: The increase in cooling due to an enhanced FIR emission is balanced by an approximately equal increase in absorbed energy. The ice mantle alters the absolute values of the far IR absorption efficiency, but not the slope β (defined by $\kappa_\nu \propto \nu^\beta$). For the very same reason does the presence of ice also not influence the derivation of the color temperature T_c.

In order to evaluate Eq.(4) we had, of course, to calculate $Q_\nu^{abs}(a)$ at *all* wavelengths, not only at $2.2\mu m$ or $1.3mm$, but the discussion of the whole spectral range is deferred to Sect. 4.

3.3. Fluffy grains

Fluffiness arises from coagulation. We consider in this section only the coagulation of one type of subparticles which may consist either of carbon or silicate; ice mantles are absent. The cross sections are presented as a function of fluffiness described by the volume fraction f_{vac} of vacuum, while the grain mass is kept fixed. Let a_s denote the grain radius when there is no vacuum inclusion ($f_{vac} = 0$). We perform calculations for $a_s = 0.1\mu m$, i.e. we consider relatively small grains well in the limits of the MRN size distribution. However, the results are quite insensitive to the particular choice of a_s. We compute cross sections in three approximate ways: from the effective medium theories after Bruggeman (BR) and Maxwell–Garnett (MG) (Sect. 2.3) and, as a third alternative, we calculate hollow spheres (see Sect. 2.3). In the MG theory, vacuum is considered to be the inclusion (although these inclusions are not separated). The ordinate in Figs. 6 and 7 has again been normalized by dividing by the cross section of a solid sphere of the same mass and chemistry.

3.3.1. The 1.3mm absorption coefficient of porous grains

Figure 6 shows the variation of $\mathscr{K}$ at $\lambda = 1.3mm$ with the degree of porosity. Moderate fluffiness in silicates with a vacuum volume fraction $f_{vac} \approx 50\%$ increases $\mathscr{K}$ about three times; in carbon with its large optical constant ($|m| \approx 20$) the excursion can be tremendous and $\mathscr{K}$ is almost 50 for $f_{vac} \approx 0.65$. Up to $f_{vac} \approx 50\%$, all three approximations yield similar results. Those for hollow particles and Maxwell–Garnett even coincide in the figure (they diverge when $a_s >> 10^{-5}\,cm$). Substantial differences between the results show up when f_{vac} becomes greater than 0.5. Generally, when the volume fraction f_i of the inclusion is very small or very close to unity the formulae of Bruggeman and Maxwell–Garnett yield the same results: in both rules $\epsilon_{av} \to \epsilon_m$ for $f_i \to 0$ and $\epsilon_{av} \to \epsilon_i$ for $f_i \to 1$. However, for $f_i \to 1$ they do not approach the limiting value with the same slope, as they do for $f_i \to 0$. Therefore the BG and MG theory may give quite different absorption coefficients for f_i values very close to 1. Treating in the Maxwell–Garnett theory the vacuum as the matrix and the grain material as the inclusion we obtain $\mathscr{K} = 1$ (not shown); the inclusions do not interact and we have the classical Rayleigh limit where the absorption cross section depends only on the mass of the material.

3.3.2. The $2.2\mu m$ extinction of fluffy grains

At $2.2\mu m$, the influence of porosity on the extinction coefficient is less severe than at $1.3mm$. Nevertheless, it must not be neglected. The effect is stronger for carbon than for silicate (Fig. 7).

3.3.3. Temperatures of fluffy grains

When we calculate how the temperature of carbon and silicate grains, immersed in the diluted black body radiation field described in Sect. 3.1.3, changes when the grains become fluffy we find that as long as the porosity is moderate ($f_i < 60\%$) the temperature does not deviate much ($< 10\%$) from that of the solid particle. For larger porosities the excursions become bigger and the results depend on the theory used. Nevertheless, we tentatively conclude that porosity does not have a strong effect on grain temperatures.

4. "Realistic" grains in stellar disks or protostellar clouds

We now return to the "realistic" grains described in Sect. 2.1. It is likely that grains in cold and dense clouds or in stellar disks have undergone all the modifications simultaneously that were treated in the previous Sect. 3, i.e. they are big, fluffy and ice coated. We show how the effects, discussed in Sect. 3 separately, add up. For this end, we display in Sect. 4.1 the cross section of such *fluffy aggregates* as a function of particle size at the two selected wavelengths $2.2\mu m$ and $1.3mm$; in Sect. 4.2 we compute their mass extinction coefficient for a size distribution over the whole wavelength range.

4.1. Cross sections in the near IR and at one millimeter

We calculate the cross section of the "realistic" grains as a function of particle size at $2.2\mu m$ and $1.3mm$ in the Bruggeman and Maxwell–Garnett theory; for the latter we assume that the most voluminous component, which is ice, forms the matrix. If M_{ref} denotes the mass of refractory material in the "realistic" grain (i.e. total particle mass minus ice mass) we normalize by the cross section of a mixture of standard dust of the same total mass M_{ref}; the standard dust consists of solid, uncoated, pure silicate and carbon grains with an MRN size distribution. Let Q_ν and a denote the absorption efficiency and radius of the fluffy grain under study, f^{Si} and f^C the volume fraction of silicate and carbon with $f^{Si}/f^C = 1.41$ (Sect. 2.1). The sum of all volume fractions is one: $f^{Si} + f^C + f^{ice} + f^{vac} = 1$. The silicate material in the fluffy grain has a volume out of which one can form $f^{Si}(a/a_{sta})^3$ standard grains of radius a_{sta}, efficiency Q^{Si}_{sta} and total cross section is $\pi f^{Si} Q^{Si}_{sta} a^3/a_{sta}$; an analogous expression holds for carbon. The normalized cross section of the "realistic" grain is therefore given by

$$\mathscr{K}_\nu(a) = \frac{Q_\nu/a}{(\frac{Q^{Si}_\nu}{a} f^{Si})_{sta} + (\frac{Q^C_\nu}{a} f^C)_{sta}} \qquad (6)$$

At $1.3mm$, the Rayleigh limit is perfectly valid with respect to standard dust and $(Q^{Si}/a)_{sta}$ and $(Q^C/a)_{sta}$ in Eq.(6) are constant, independent of the size of the standard grain. We use $(Q^{Si}/a)_{sta} = 1.00$ and $(Q^C/a)_{sta} = 1.22$ (a in cm). At $2.2\mu m$, where absorption *and* extinction cross section have to be evaluated, the denominator in Eq.(6) is only approximately constant and varies by 20% from small (100Å) to large (2000Å) standard grains. We nevertheless employ Eq.(6) and use as averages over the size distribution of the standard dust: $(Q^{Si}/a)_{sta} = 1800$ and $(Q^C/a)_{sta} = 2000$ (a in cm) for both absorption and extinction.

Figure 8 gives the result for the $1.3mm$ absorption coefficient in the Bruggeman theory for several combinations of parameters. To better visualize their influence we always compare with a reference case (solid line) for which we choose: $M_{ice}/M_{ref} = 1$, a vacuum fraction $f_{vac} = 0.5$, and an optical constant of ice $k_{ice} = 0.02$. We vary M_{ice}/M_{ref} from 0.5 to 1.5, k_{ice} from 0.01 to 0.03 and f_{vac} between 0.3 and 0.7. The limits for the mass fraction of ice are certainly very reasonable (Sect. 2.1), probably also those for k_{ice} (Sect. 2.2); however, the upper boundary of $f_{vac} = 0.7$ is motivated rather by the diverging outcome from different theories if f_{vac} is large (Fig. 6). We also crudely simulate a fractal structure by considering a grain that is more fluffy at its edge than in its core: We take $f_{vac} = 0.3$ for the inner 80% of grain radius, corresponding to half the grain volume, and $f_{vac} = 0.7$ outside. Such a structure is described by a fractal dimension $D = 1.53$ (for compact spheres: $D = 3$).

All curves in Fig. 8 have similar shape: the normalized absorption cross section is constant up to $a = 100\mu m$; it rises and reaches its maximum for particles with a diameter of about 1mm and falls again at very large radii. In the scenarios of Fig. 8, $\kappa_{1.3mm}$ is between six and fourteen times greater than in the diffuse interstellar medium as long as $a \leq 100\mu m$; for the reference case this factor is eight. So the specific choice of M_{ice}/M_{ref}, f_{vac} and k_{ice} does not have a dramatic effect, at least, if the parameters are varied within the range treated in Fig. 8.

In Fig. 9 we repeat the calculations of Fig. 8 using this time the Maxwell–Garnett rule, ice being the matrix. Fortunately, the results agree quite well for the two rules. We note, however, that the Maxwell–Garnett theory gives values of $\mathscr{K}_{1.3mm}$ that are enhanced up to a factor of three if we choose the refractory material for the matrix.

In a qualitative way, the discussion for the normalized extinction coefficient $\mathscr{K}^{ext}_{2.2\mu m}$ at $2.2\mu m$ is similar (Figs. 10 and 11) if one scales with the size parameter $2\pi a/\lambda$. For grain radii $a \leq 0.2\mu m$ we find an almost twofold increase with respect to the diffuse interstellar medium, for micron sized grains it can be an order of magnitude. The Bruggeman and Maxwell–Garnett theory give again very compatible results.

4.2. The mass extinction coefficient of fluffy aggregates with a size distribution

We now study the mass extinction coefficient of the fluffy aggregates taking into account a grain size distribution $n(a)$. As we have at present no clue for its shape we assume that $n(a)$ follows the same power law as the standard dust in the diffuse medium (MRN mixture), i.e. $n(a) \approx a^{-q}$ with $q = 3.5$. The MRN mixture has an upper size limit $a_+ \approx 0.3\mu m$ and a lower $a_- \approx 100$Å. We adopt for the fluffy aggregates a larger value of a_- to account for the removal of very small grains from the size spectrum by coagulation in dense regions; we take $a_- = 300$Å. The upper limit is considered a free parameter and we vary a_+ from $0.3\mu m$ to 3mm. Results are summarized in Fig. 12. The standard curve for the diffuse medium is displayed for comparison and marked MRN. We recall that for large wavelengths, $\lambda >> a$, extinction and absorption cross section are about equal.

First, we turn our attention to the curve refering to fluffy aggregates with $a_+ = 0.3\mu m$ (dashed). Although it has a similar size distribution as the MRN grains, it gives very discrepant values: *a)* there are prominent ice resonances at 3.1, 14 and 46 μm; they tend to swamp the silicate features at $9.7\mu m$ and especially at $18\mu m$; *b)* the extinction cross section is enhanced everywhere; the increase amounts to a factor of 1.5 at $2.2\mu m$ and to one order of magnitude in the entire FIR/submm region; *c)* with regard to the dependence of the extinction coefficient

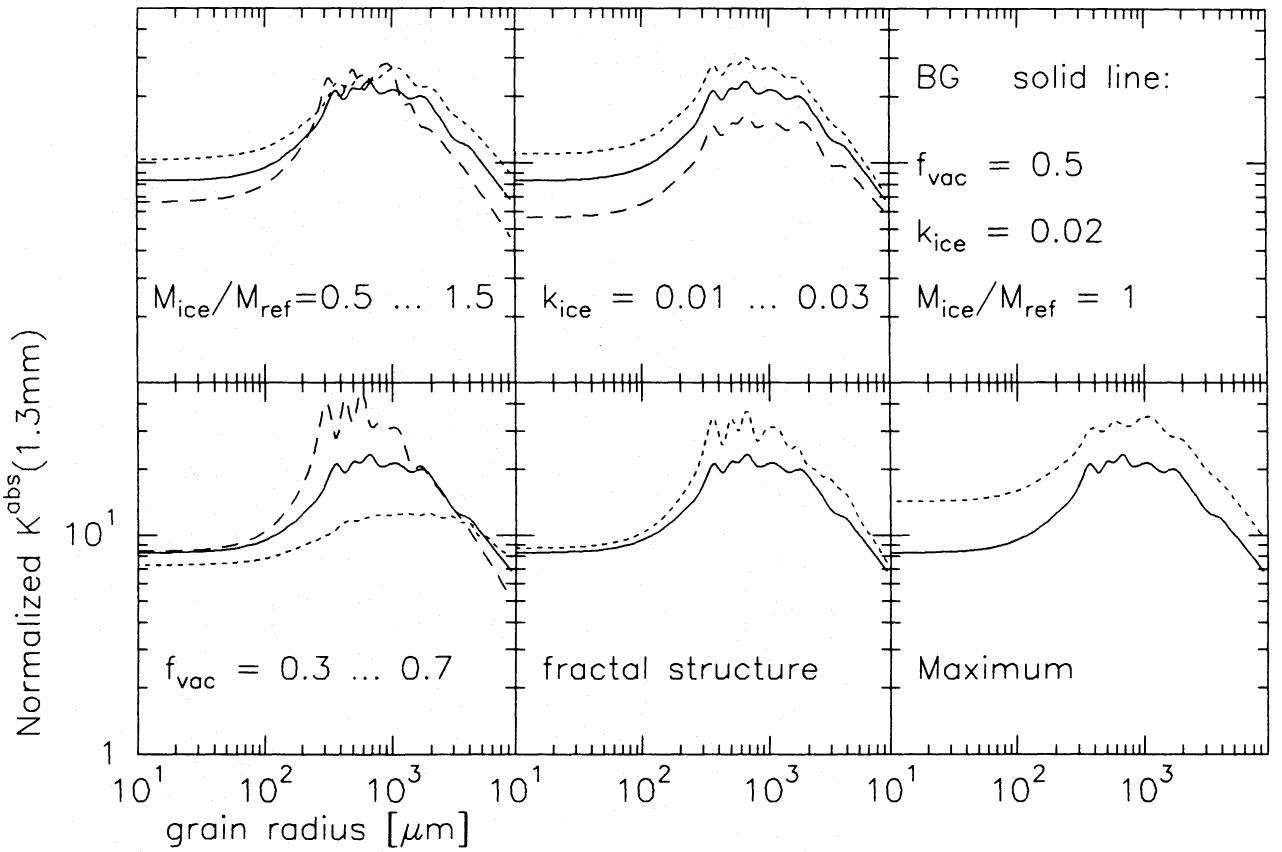

Fig. 8. Normalized absorption cross section at 1.3mm of "realistic" fluffy particles as a function of grain radius. The grain is porous and composed of silicate and carbon (total refractory mass M_{ref}), ice (mass M_{ice}) and vacuum. The volume fraction of silicate and carbon is constant with $f^{Si} = 1.41 \cdot f^{C}$. Calculations are performed with the Bruggeman mixing rule; for normalization see Sect. 4.1. In each frame, the solid line shows the reference case: $M_{ice}/M_{ref} = 1$, $k_{ice} = 0.02$, $f_{vac} = 0.5$ and constant internal density. We vary: **a)** M_{ice}/M_{ref} from 0.5 (dashed) to 1.5 (dotted); **b)** k_{ice} from 0.01 (dashed) to 0.03 (dotted); **c)** f_{vac} from 0.3 (dashed) to 0.7 (dotted); **d)** the fratcal structure, the dotted line refering to a particle where the core has $f_{vac} = 0.3$ and the shell $f_{vac} = 0.7$. In the frame labelled "Maximum", the dotted curve has $f_{vac} = 0.5$ and values which tend to maximize the absorption coefficent: $M_{ice}/M_{ref} = 1.5$, $k_{ice} = 0.03$. For normalization see Sect. 4.1

on wavelength, $\kappa^{ext} \propto \nu^{-\beta}$, the exponent β is at submm wavelengths not far from 2 and similar to the MRN curve. A closer inspection shows that the curve is flattening at 1mm.

If $a_+ = 30\mu m$ (dotted line), the qualitative behavior at submm/mm has not changed at all. This is noteworthy because the upper size limit has increased a hundred times and still bigger grains should be reserved to very special environments. In the FIR around $\lambda \simeq 100\mu m$, β is now slightly *larger* than 2, but not much. All ice features have more or less disappeared. The slope of the extinction coefficient changes fairly abruptly at $\lambda = 30\mu m$ from $\simeq 2$ at long wavelengths to a very constant $\beta \simeq 0.4$. In the UV and visible, the extinction is now smaller than for the MRN curve and the intersection occurs approximately in the J–band ($1.2\mu m$).

Finally, if $a_+ = 3$mm, as is realistic for Vega–type stars and possibly disks around young stellar objects, we find that $\beta \simeq 0.4$ over the entire spectrum; one begins to approach the value of a black body ($\beta = 0$). However, in Vega–type stars very simple dynamical arguments show that radiation pressure and the Poynting–Robertson should clear the stellar environment from very small grains unless there exists a constant fresh supply. This was corroborated independently from models fits to the IR spectra of these stars (see the fit to β Pic in Fig. 1e and 1f of Chini et al. 1991). So in Vega–type stars a_- is certainly larger than $1\mu m$ (for a grain size distribution is $n(a) \propto a^{-3.5}$) and we therefore also give in Fig. 12 the curve marked "β Pic" where $a_+ = 3mm$, but $a_- = 30\mu m$ in qualitative accordance with the fit results of Chini et al. The slope of the absorption coefficient is now completely flat even in the far IR out to $100\mu m$; the systematic trend continues that, except for the longest wavelengths, κ declines with increasing particle size.

5. Discussion

5.1. Trustworthiness of the results

Several articles have addressed the question of the validity of effective medium theories (EMT). Their reliability is usually evaluated by comparison with other methods that can also handle fluffy particles, in particular with the discrete dipole approximation (DDA) (Purcell & Pennypacker 1973; Draine 1988; Perin

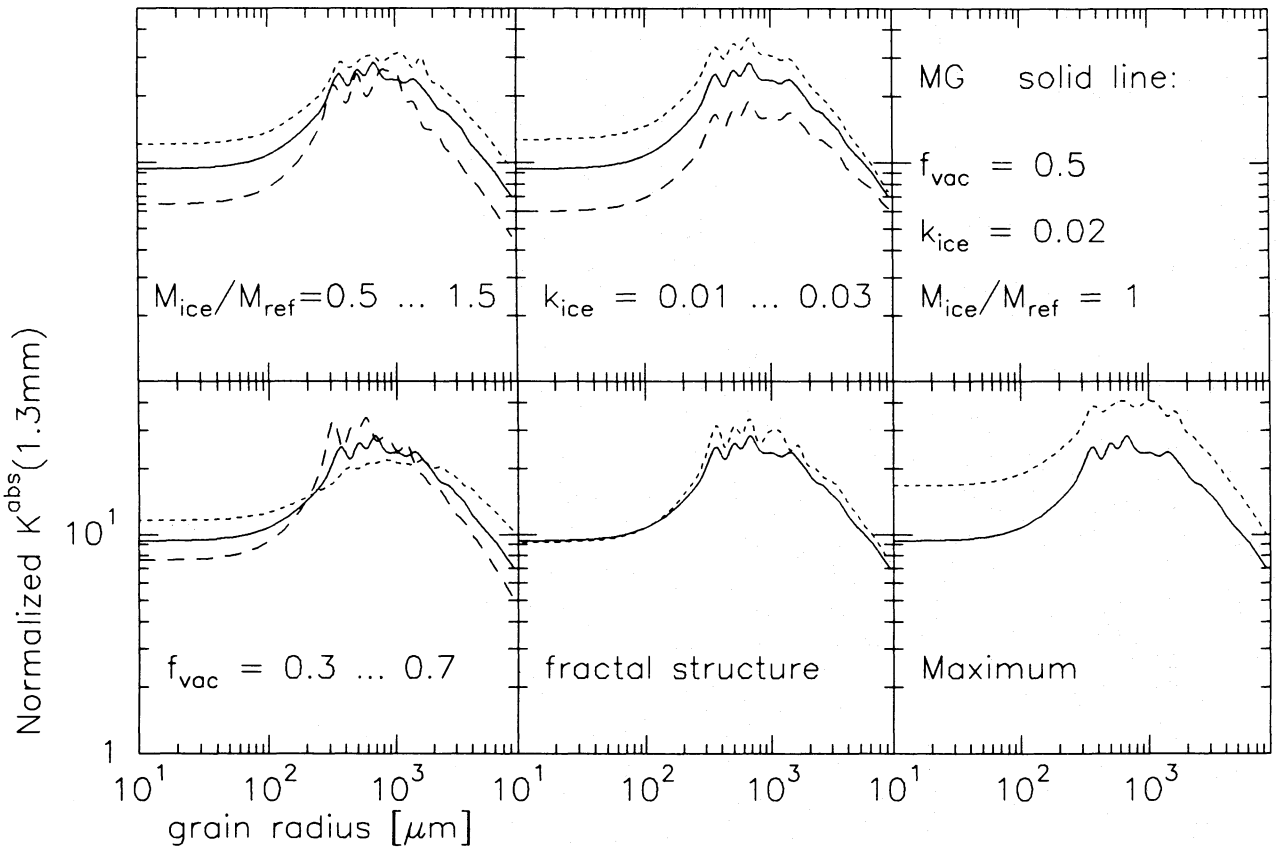

Fig. 9. As Fig. 8, but with the Maxwell–Garnett theory, ice being the matrix.

& Lamy 1990; Draine & Goodman 1993). The DDA is certainly more versatile and is thought to be more correct. In its numerical treatment, the fluffy particles are represented by a collection of homogeneous subvolumes or dipoles mounted in a cubic lattice with a spacing small compared to the wavelength. This has the unpleasant consequence of large amounts of computing time. Furthermore, one is faced with the problem of having to specify the virtually unknown grain substructure. In practice, only randomly produced networks are used. For simple geometries, such as spheroids, results from Mie theory are successfully reproduced by the DDA. Mukai et al. (1993) found good agreement for absorbing materials and compact structures. Perrin & Lamy (1990) noticed a deviation in the extinction cross section near the 9.7 μm Si–O feature of about 30%, however, neglecting shape effects. Ossenkopf (1991) could reduce the discrepancy for this case by taking geometry factors explicitly into account. Recently, another method to handle inhomogeneous grains was proposed by Hage & Greenberg (1990). It consists of an integral representation of Maxwell's equations. These authors could also confirm the approximate validity of the EMT. With respect to the question which of the most commonly EMTs should be applied, Maxwell–Garnett or Bruggeman, there is presently no clear answer, neither from theory nor from laboratory data. We found for "moderate" grain configurations satisfactory agreement between both mixing rules if we choose in the Maxwell–Garnett theory ice for the matrix, which is the material with the largest volume fraction. (see Figs. 6 to 11).

Our results are, at least, qualitatively in accord with previous papers on fluffy grains. There is general agreement that porosity significantly enhances the absorption efficiencies at far IR and submillimeter wavelengths and that compositional inhomogeneities have a large effect on the shape and strength of broad band features (Bazell & Dwek 1990; Perrin & Lamy 1990; Ossenkopf 1991; Preibisch et al. 1993). Recently, an attempt was made by Ossenkopf (1993) to elucidate the structure of fluffy grains by studying the processes that lead to coagulation. He created fluffy particles in computer simulations of ballistic encounters and calculated their cross sections by applying effective medium theories. His approach is different from ours in the sense that we treat the basic particle properties, like fluffiness and size, as free parameters and investigate their influence on the dust cross section; we do not embark on the formidable task of giving a physical explanation for their particular choice.

5.2. *Protostellar clouds*

In the exciting search for early phases of star formation, the decision whether a cold cloud fragment without a detectable embedded star can be considered a protostellar candidate hinges on the question whether the gas mass exceeds the critical limit for gravitational instability or not. As molecular lines can be-

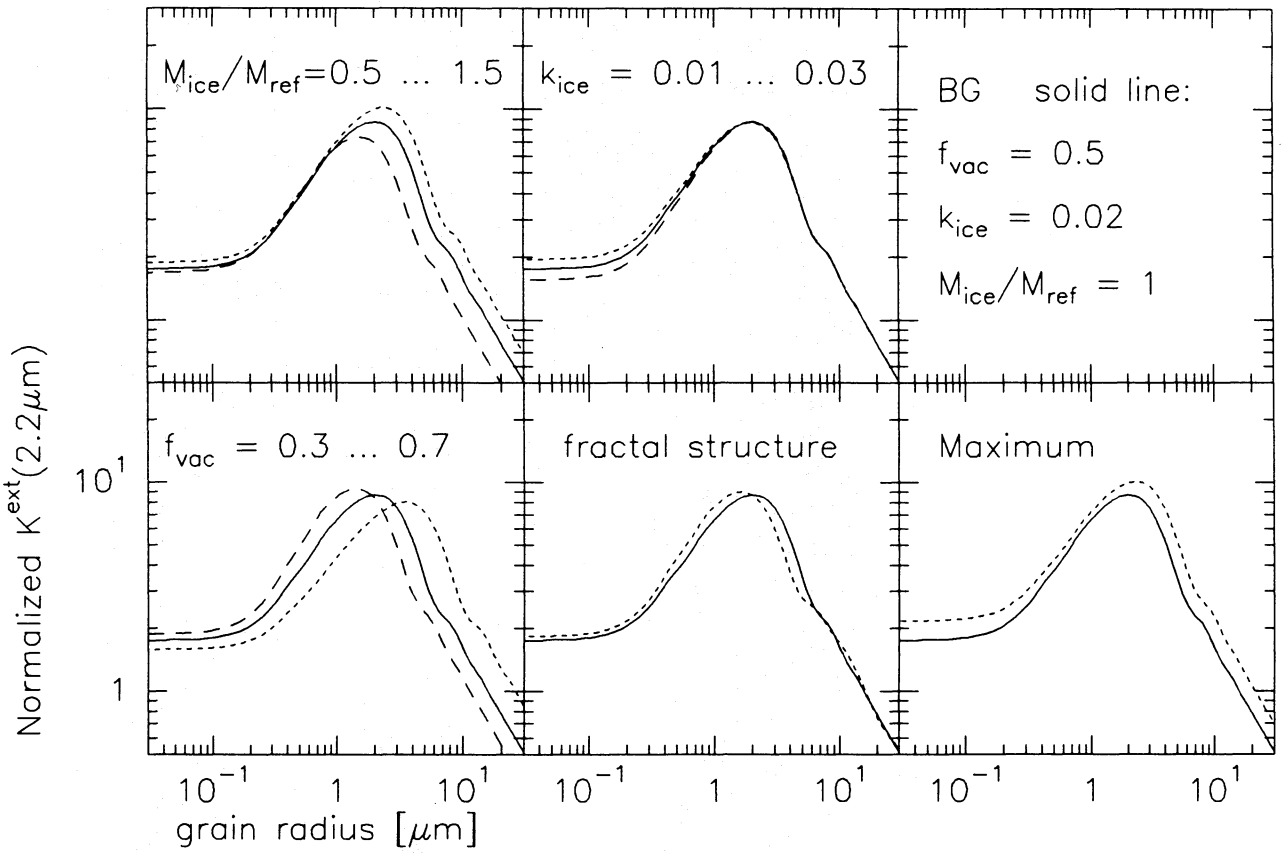

Fig. 10. Normalized extinction cross section at 2.2 μm using Bruggeman theory, otherwise as Fig. 8

come unreliable as mass tracers due to frosting and details of chemistry there is the need for sound mass estimates from dust emission and thus for a good value of $\kappa_{1.3mm}$.

An example which stresses this need and also suggests that coagulation of grains actually does take place in cold and dense clouds is presented by the source named HH24 MMS. This object is a good candidate for a protostellar cloud because it is very compact and cold ($T_d \approx 10K$) (Chini et al. 1993). Using the standard absorption coefficient of the interstellar medium at $1.3mm$ one derives for HH24 MMS from dust emission a gas mass $M_g(dust)$ that is uncomfortably high. It exceeds the mass obtained from optically thin $C^{18}O$ by a factor of 250 (Krügel & Chini 1994). Of course, frosting may have reduced the number of molecules in the gas phase, but this cannot be the sole explanation: Interpreting the $C^{18}O$ line width as a virial velocity still gives a mass that is twenty times smaller than $M_g(dust)$, although such an estimate is independent of the degree of molecular depletion. Therefore $M_g(dust)$ must be a gross overestimate. In cold and dense clouds there are probably two effects at work which tend to distort mass derivations: molecular underabundance in the gas phase and an enhanced dust emissivity at 1mm. As it is likely that in HH24 MMS the grains have coagulated and formed ice mantles, we expect from the results of Figs. 8 and 9 a tenfold increase in $\kappa_{1.3mm}$. This would reconcile the mass estimates and reduce the discrepancy between $M_g(dust)$ and the virial mass into the range of normal scatter; we note that Jeans' criterion for instability would still be fulfilled for this source.

Another important consequence of modified cross sections through fluffy aggregates concerns the visibility of embedded protostars. The value of $\kappa^{ext}_{2.2\mu m}$ determines in an extremely sensitive way the chances for detecting a source because of the exponential dependence of the emerging flux on the optical depth ($S \propto e^{-\tau}$). Even small changes in $\kappa^{ext}_{2.2\mu m}$ will produce dramatic effects once τ is, say, greater than 5. As grain growth in a collapsing protostellar cloud proceeds gradually we conclude from Figs. 10 and 11 that coagulation will first increase the optical depth and thus hide near IR sources in protostellar clouds that would otherwise be visible had the dust the properties of the diffuse medium. Details are complicated and depend also on the ratio of coagulation time τ_{coag} over free–fall time τ_{ff}. If particles with radii larger than $0.3\mu m$ have formed, $\mathscr{K}$ may be both above and below unity; the net effect on the $2.2\mu m$ extinction depends then on the size distribution, i.e. if it is a power law, on the upper and lower limit and the exponent.

5.3. Protostellar disks around low mass stars

In a study of T Tau stars, Beckwith et al. (1990) argue that the circumstellar material is concentrated in a disk. They fit spectra to the disks and derive their masses, mainly from the $1.3mm$ emission by adopting $\kappa_{1.3mm} = 0.02\,cm^2$ per g of interstellar

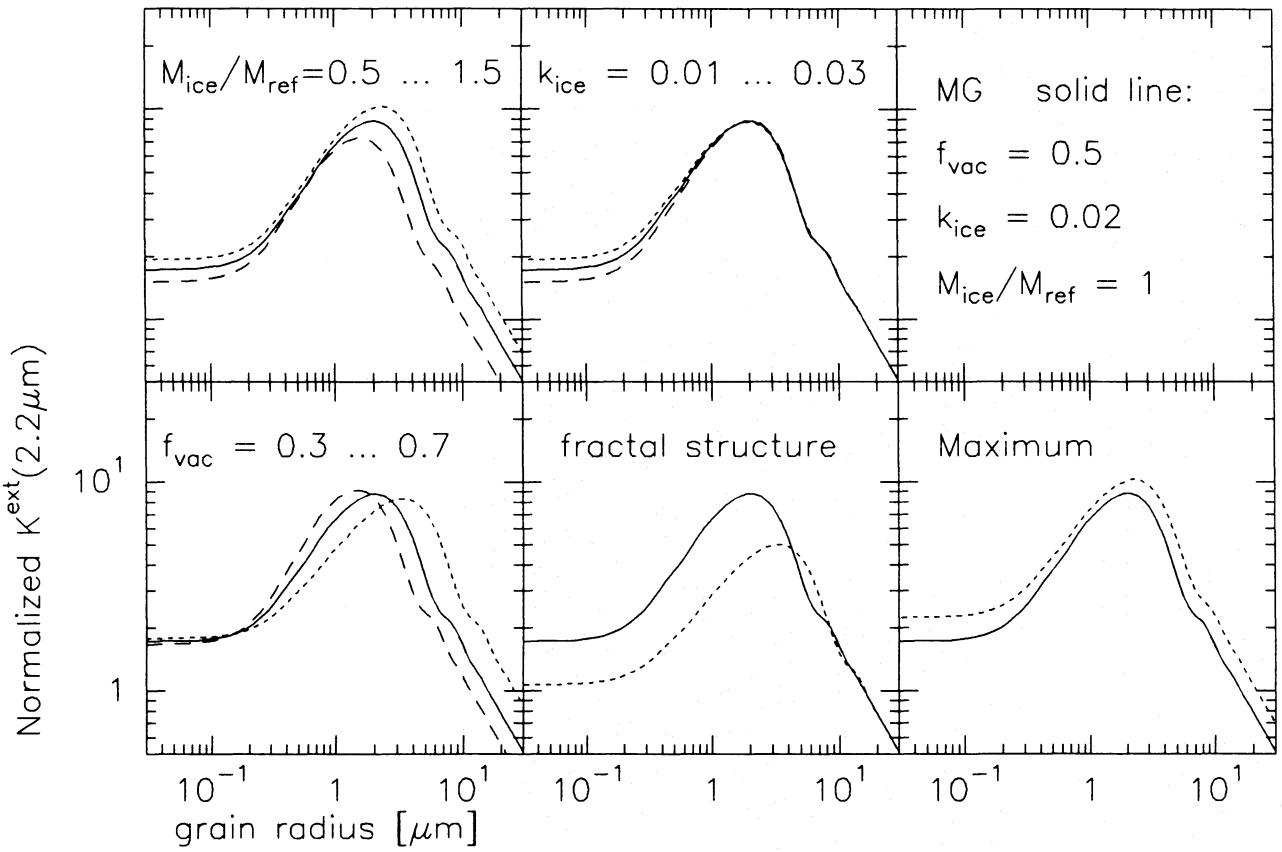

Fig. 11. Normalized extinction cross section at 2.2 μm using Maxwell–Garnett theory, the ice matrial forms the matrix, otherwise as Fig. 8

matter and $\beta = 1$; these numbers were taken from suggestions by Hildebrand (1983) and Wright (1987) for fluffy particles. The value $\kappa_{1.3mm} = 0.02\, cm^2$ of Beckwith et al. is a factor of eight larger than for the diffuse ISM (see MRN curve in Fig. 12); it is in agreement with our calculations for fluffy aggregates (dotted and dashed lines in Fig. 12) provided the grains in the disk are not extremely big ($a_+ > 30\mu m$) and their temperatures stay below the evaporation of ice ($\simeq 100K$). However, in our dust model the value of $\kappa_{1.3mm} = 0.02\, cm^2/g$ implies that β is close to 2 (Fig. 12), and not one; $\beta = 1$ would result in fits to spectra of T Tau stars that have quite different parameters (disk structure) than those of Beckwith et al. (1990).

5.4. Disks around Vega–type stars

These stars discovered by IRAS (Aumann et al. 1984) lie on the main sequence and possess a far IR excess over the black body emission of their photosphere. Additionally, in the case of β Pic there is a sharp disk of scattered star light at optical wavelengths (Smith & Terrile 1984). The IR excess could be successfully interpreted to be due to emission of much larger–than–normal dust grains ($a \geq 10\mu m$). Roughly speaking, observations at a wavelength λ are most sensitive to grains of size $2\pi a = \lambda$. Therefore Chini et al. (1991) could conclude from their measurements at $1.3mm$ that the largest particles must be, *at least*, several millimeters in diameter. This implies that even at $\lambda = 1.3mm$ the Rayleigh limit ($a << \lambda$) is not valid and the absorption coefficient depends explicitly on grain size; one is no longer in the flat section of the curves in Figs. 8 and 9. If the grain size distribution around Vega–type stars has the canonical power law exponent $q = -3.5$, then the mass is contained in the biggest particles. Should a_+ be greater than several millimeters then they would not be visible (planets ?) and all mass estimates are only lower limits.

6. Conclusion

1. We investigate how the absorption and extinction cross section of dust depend on the size of the grains, their porosity and the presence and absorbing proprties of an ice mantle. In detail we present results for $\lambda = 1.3mm$, widely used in mass estimates, and for $\lambda = 2.2\mu m$, appropriate in searches of obscured young stars. They are expressed by a normalized cross section which gives directly the change relative to the standard dust in the diffuse interstellar medium. We find:

i) The grain radius a has a tremendous effect on the cross section when it becomes comparable to the wavelength, ($2\pi a \simeq \lambda$). For very large particles, ($a >> \lambda$), κ will be very small. Details depend on the particular wavelength and the optical constants of the material (see Figs. 1 and 2).

ii) An ice coating always increases the extinction coefficient. The problem is to determine the appropriate degree of pollution

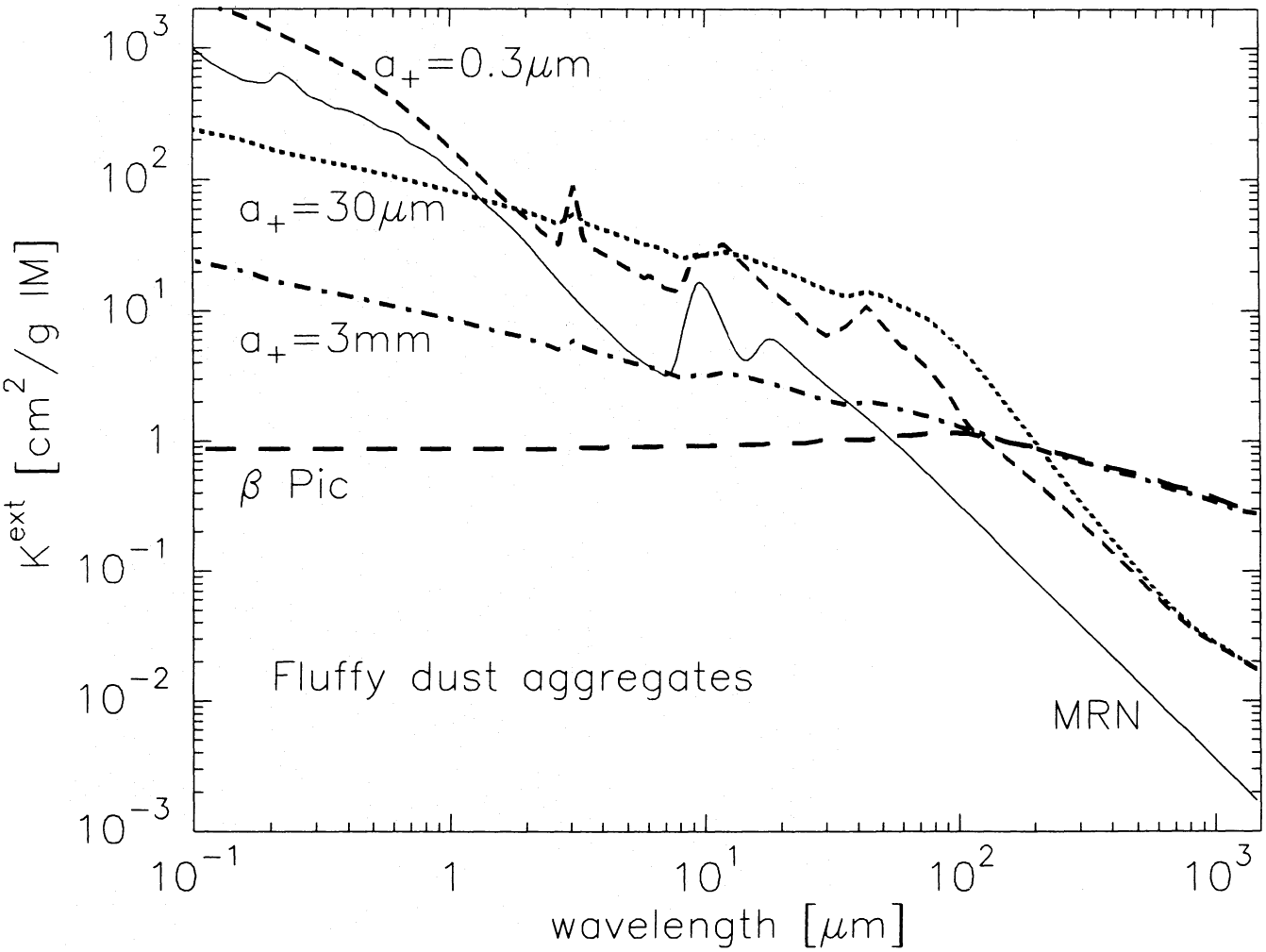

Fig. 12. Mass extinction coefficient as a function of wavelength for a mixture of "realistic" grains with a size distribution $n(a) \propto a^{-3.5}$. The grains are composed of silicate, carbon ice and vacuum and they are the fluffy aggregates described in Sect. 2.1. (M_{ice}/M_{ref} = 1 and f_{vac} = 0.5). The cross sections are calculated with the Bruggeman mixing rule. The lower limit a_- of the size distribution is 300Å, the upper limit a_+ is indicated. The curve labeled "β Pic" has a_- = 30μm and a_+ = 3mm. For comparison, we show the standard curve (MRN) of the diffuse ISM which has a_- = 100Å and a_+ = 0.3μm. We suggest that the curve labeled a_+ = 0.3μm is applicable to the dust in a dense molecular cloud or a disk around a YSO

of the ice, expressed by the imaginary part of the optical constant. At 2.2μm and 1.3mm, we suggest $k_{ice} \simeq 0.02$ (Figs. 4 and 5).

iii) Porosity also enhances the absorptivity. As it implies an inhomogeneous grain structure one has to use an approximate method for calculating cross sections. If the volume fraction of vacuum is moderate ($\leq$ 70%) different methods yield similar results (Figs. 6 and 7).

2. We calculate at λ = 2.2μm and λ = 1.3mm the normalized cross section of *fluffy aggregates* composed of silicate, carbon, dirty ice and vacuum. Such structures are more realistic for protostellar environments and dusty disks. The basic parameters of such grains are size, volume fraction of vacuum, mass fraction of ice, impurity of ice, and fractal dimension (Figs. 8 to 11). These parameters are varied over a reasonable range .

3. Taking into account a size distribution $n(a) \propto a^{-3.5}$ of the fluffy aggregates, we evaluate the mass extinction coefficient of such an ensemble of "realistic" particles over the whole wavelength range from 0.1 to 2000μm. The particles have a fixed minimum radius, a_- = 0.03μm and the upper limit a_+ is treated as a parameter. Figure 12 allows to read off the extinction coefficient as a function of wavelength for dust in various environments.

4. The structural differences of dust in a dense environment also affect the true temperature T_d of the grains and the color temperature T_c that would be derived from observed submm flux ratios. The grain size can greatly distort both values. The influence of porosity and the presence of ice material seem less grave.

5. We discuss as an application protostellar clouds and stellar disks. We propose for the cold cores of protostellar clouds a mass

absorption coefficient $\kappa_{1.3mm} = 0.02\,cm^2$ per g of interstellar matter and $\beta = 2$ for the dependence of κ on wavelength in the submm region ($\kappa \propto \nu^{-\beta}$). If ices have not evaporated, $\kappa_{1.3mm}$ may be similar for disks around young stars. The dust in Vega–type stars constitutes a class of its own, where the grains are probably still icy, but extremely large. The curve labelled "β Pic" in Fig. 12 may be applicable.

Acknowledgements. We are much indebted to the referee, Dr. V. Ossenkopf, for helpful criticism and also to Dr. Th. Preibisch.

References

Allamandola L.J., Tielens A.G.G.M., Barker J.R., 1989, ApJ Suppl 71, 733
Aumann H., Gillet F., Beichman C. et al., 1984, ApJ 278, L23
Bazell D., Dwek E. 1990, ApJ 360, 142
Beckwith S.V.W., Sargent A.I., Chini R., Gusten R., 1990, AJ 99, 924
Bertie J., Labbe H. Whalley E., 1969, J. Chem. Phys. 50, 4501
Blanco A., Fonti S., Rizzo F., 1991, Infrared Phys. 31, 167
Blum J., Henning Th., Ossenkopf V., Sablotny R., Stognienko R., Thamm E., 1993, A&A in press
Bohren & Huffman D.R., 1983, Absorption & Scattering of Light by Small Particles, John Wiley & Sons, New-York – Chichester – Brisbane – Toronto – Singapore
Bussoletti E., Colangeli L., Borghesi A., Orofino V., 1987, A&A Suppl. 70, 257
Chini R., Krügel E., Shustov B., Tutukov A., Kreysa, E., 1991, A&A 252, 220
Chini R., Krügel E., Haslam C.G.T. et al., 1993, A&A 272, L5
Chokshi A., Tielens A.G.G.M., Hollenbach D., 1993, ApJ 407, 806
van Dishoeck E.F., Blake G.A., Draine B.T., Lunine J.I., 1993, in: Protostars & Planets III, Levy E.H., Lunine J.I., Matthews M.S. (eds.),Univ. Arizona Press, Tucson
Draine B., 1985, ApJ Suppl 57, 587
Draine B., 1988, ApJ 333, 848
Draine B., Goodmann, 1993, ApJ 405, 685
Edoh O., 1983, PhD. Thesis, University of Arizona
Hage J.I., Greenberg J.M., 1990, ApJ 361, 251
Hildebrand R.H., 1983, R. Astron. Soc. 24, 267
Jones, A.P., 1988, MNRAS 234, 209
Kerker M., 1969, *Scattering of Light*, Academic Press, New York and London
Kozasa, T., Blum J., Mukai, T., 1992, A&A 263, 423
Krügel E., Chini R., 1994, A&A (in press)
Lada C.J., Adams F.C., 1992, ApJ 393, 278
Leger A., Gauthier S., Defourneau D., Rouan D., 1983, A&A 117, 47
Mathis J.S., Rumpl W., Nordsieck K.H., 1977, ApJ 217, 425
Mathis J.S., Whiffen G., 1989, ApJ 341, 808
Meakin P., Donn B., 1988, ApJ 329, L39
Morfill G.E., 1984, The 27th International Geological Congress, Tom 5, p.352
Ossenkopf V., 1991, A&A 251, 210
Ossenkopf V., 1993, A&A 280, 617
Perrin J.M., Lamy, P.L., 1990, ApJ 364, 146
Purcell E.M., Pennypacker C.R., 1973 ApJ 186, 705
Preibisch Th, Ossenkopf V., Yorke H.W., Henning Th., 1993, A&A 279, 577
Rouleau F., Martin P.G., 1991, ApJ 377, 526
Smith B., Terrile R., 1984, Sci 226, 1421
Tielens A.G.G.M., Tokunaga A.T., Geballe T.R., Baas F., 1991, ApJ 381, 181
Whittet D. 1993, *Dust and Chemistry in Astronomy*, eds. R. Tayler & R. White, p.9
Witten T.A., Cates M.E., 1986, Science 232, 1607
Wright E., 1987, ApJ 320, 818
Wright, E., 1988, ApJ 337, L41

This article was processed by the author using Springer-Verlag LaTeX A&A style file version 3.